

Performance Assessment of a 3 DOF Differential Based Waist joint for the “iCub” Baby Humanoid Robot

W. M. Hinojosa, N. G. Tsagarakis, G.Metta, F.Becchi, G.Sandini and D. G. Caldwell

Abstract— This work discusses the design and control approach of a 3 DOF waist joint for the “iCub” humanoid robot. “iCub” is a child like crawling robot that resembles a 2 and a half year old child. The ultimate goal of this project is to provide the cognition research community with an open human like platform for understanding of cognitive systems through the study of cognitive development. The designs of the mechanisms adopted for the waist joint are discussed. This is accompanied by discussion of the control scheme design and presentation of experimental results showing the performance of the mechanism.

I. INTRODUCTION

Anthropomorphic type robots combine many desirable features such as natural human like locomotion and human friendly design and behavior. As a result of this multi degree of freedom human like robots have become more and more common and many humanoid robots have recently been designed and fabricated.

The first biped humanoid robot was WABOT developed at Waseda University in 1973. This biped which was able to perform simple static walking was followed by the development of WABIAN I and II. WABIN-RII[1]. Following these first prototypes a number of other human like robots were developed including the H6, H7 at the University of Tokyo [2], the impressive humanoid robots P2, P3 and ASIMO developed by HONDA [3-5] and some more recent prototypes such as the JOHNNIE the anthropomorphic autonomous biped robot [6] developed at University of Munich and the HRP, HRP-2 developed by METI in Japan [7-10].

Other less well know medium and small size humanoids include SAIKA [11] and KENTA [12], the MK.5 a compact size humanoid robot constructed by Aoyama Gakuin University [13], the PINO platform constructed by ERATO [14] and the SDR-3X (Sony Dream Robot-3X) and SDR-4X

developed mainly for entertainment [15, 16].

In the above examples the waist joint is usually implemented using a simple serial mechanism with 2 DOF. This waist configuration is adequate for these robots since the tasks that are usually performed are limited to entertainment and amusement applications and in demonstrating walking capabilities.

The concept behind the development of iCub is to provide the cognition research community with an open architecture human like hardware/software platform for understanding of cognitive systems through the study of cognitive development. The iCUB will replicate a 2 and a half year old human baby acting in cognitive scenarios, performing tasks useful to learning and interacting with the environment and humans. In the early definition of the project two main tasks were considered from which the design requirements for the waist mechanism were derived. These are crawling and manipulation [17]. Based on the requirements implied by these two tasks the design of the waist mechanism of the iCub was realized. A 3 DOF differential based mechanism was employed to provide not only increased stiffness but also increased range and flexibility of motion for the upper body.

This paper presents the design and control of this differential based waist mechanism of the iCub. The paper is organized as follows: Section II gives the general specifications of the waist joint in terms of DOF, range of motions and torque requirements. The following section describes the mechanical design adopted for the waist mechanism and highlights the advantages of this approach. Section IV introduces the system model used for the design of the control scheme while section V presents the control system design. Estimated performance measures of the control scheme are presented in sections VI and VII, by means of simulation and experimental result. Finally, section VIII introduces the conclusions of this work

II. WAIST SPECIFICATIONS

The kinematics specifications of the waist joint of the iCub include the definition of the number of D.O.F required and their actual location as well as the range of motions. These were defined with attention given to address the requirement for crawling and manipulation and in general to imitate the human baby form. As has been mentioned the iCub will have the approximate size of a two and a half year old child [17]. The D.O.F required for the waist was

W. M. Hinojosa is with the Centre for Robotics & Automation (IRIS), School of Computing Science and Engineering, The University of Salford, Salford, Greater Manchester M5 4WT, United Kingdom (e-mail: W.M.Hinojosa@pgt.salford.ac.uk).

N. G. Tsagarakis is with the Centre for Robotics & Automation (IRIS), School of Computing Science and Engineering, The University of Salford, Salford, Greater Manchester M5 4WT, United Kingdom (e-mail: N.Tsagarakis@salford.ac.uk).

D. G. Caldwell is with the School of Computing Science and Engineering, The University of Salford, Salford, Greater Manchester M5 4WT, United Kingdom (e-mail: D.G.Caldwell@salford.ac.uk).

determined by considering both crawling and manipulation scenarios. Crawling simulation analysis showed that for effective crawling a 3 D.O.F waist is essential, Table I.

TABLE I
WAIST MECHANISM NUMBER OF DOFS

Joint	Degrees of Freedom (°)	
	Human	iCub
Waist	3	3
	Roll	Roll
	Pitch	Pitch
	Yaw	Yaw
		=3DOF

An additional advantage that a 3 D.O.F waist will offer is the increased range and flexibility of motion for the upper body. This increased flexibility results in an amplified workspace of the iCub when performing manipulation tasks using its hands when in a sitting position. As manipulation is directly related to learning which is an essential task for the iCub the 3 D.O.F waist will provide significant benefits. Based on the above the iCub waist needs to provide 3 D.O.F enabling pitch, roll and yaw of the upper body.

As the iCub is a human-like robot and will perform tasks similar to those performed by a human, the range of motions of a standard human were used as a starting point for the selection of the movable ranges for the waist joints of the iCub.

Table II below introduces the range of motion specifications for the joints of the waist mechanism in comparison with the corresponding ranges found in the human.

TABLE II
range of motion of the waist joint

Waist Joint	Range of motion (°)	
	Human	iCub
Waist roll	-35, +35	-90,+90
Waist pitch	-30, +70	-10,+90
Waist yaw	-40, +40	-60,+60

Looking at Table II it can be observed that the range of motion in some joints has been extended or modified. In particular, the range of the waist yaw and roll has been increased while the range of the pitch motion was modified to increase the upper body forward angle to improve the front workspace of the robot. This extends the area where the iCub can reach and manipulate objects.

The last specifications to be discussed are the required torques for the waist mechanism. This forms the starting point for the selection of the actuation groups. To optimize the selection of actuators and reduction ratios, iterations of the mechanical design of the waist and simulated analysis of the system were carried out.

The selection of the type of actuator to power the waist of the iCub involved simulations of the robot while performing crawling motions with different speeds and transitions from

a sitting to crawling pose and vice versa. From these simulations, the peak torque requirements of each joint of the waist mechanism were identified as presented in Table III.

TABLE III
TORQUE REQUIRED FOR THE WAIST MECHANISM

Waist joint	Torque Required(Nm)
Roll	30.1
Pitch	45.8
Yaw	27.2

III. WAIST MECHANICAL DESIGN

The CAD model and the first prototype of the waist mechanism of the iCub baby humanoid robot are shown in Figure 1 and 2. The iCub waist was designed using the 3D CAD software *Pro Engineer Wildfire 2* from PTC.

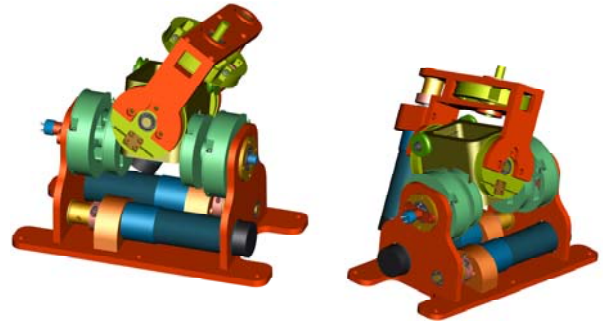


Fig. 1. CAD captures of the differential drive to be used as the robot waist.

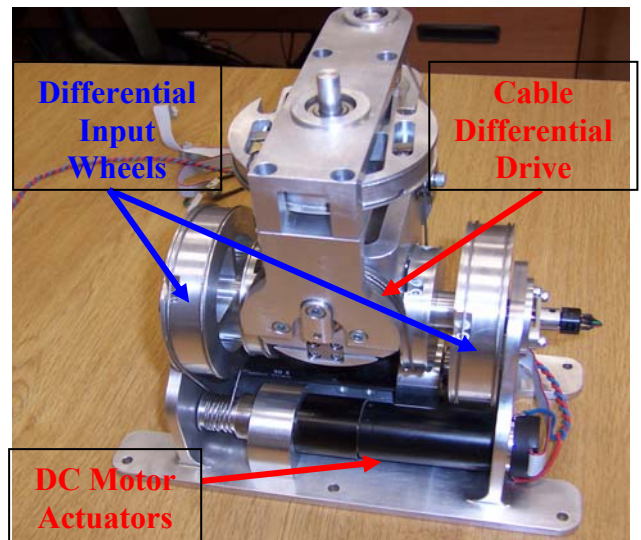


Fig. 2. Prototype of the differential based waist mechanism.

In the previous section, the role of the waist joint in the flexibility of motion of the upper body was highlighted. Such flexibility must be accompanied by high positional accuracy of the upper body as is required during manipulation.

For the pitch motion of the waist, the two actuator groups that power the pitch and yaw motion apply a synchronous motion to the two differential input wheels using the torque of both motors. For the yaw motion, the motors turn in

opposing directions. This causes a yaw motion on the upper body, again using the torque of both motors.

This differential mechanism has several advantages when compared with traditional serial mechanisms used in humanoid robots. These are:

- i) Increased stiffness and accuracy.
- ii) The sum of the torque generated by the two actuators that power the differential joint can be distributed in both joints.
- iii) As a result, smaller actuators can be used to achieve the maximum output torques required for the pitch and yaw motions.

The roll motion is implemented with the incorporation of a pulley shaft that is directly connected to the upper body frame. Torque is conveyed through a cable transmission system that provides also additional gearing to meet the torque requirements of the roll joint, Table III. For the first prototype DC motor actuators were employed to power the waist joints.

IV. SYSTEM MODEL

In order to achieve effective control of waist motions an accurate model of the system has been developed and extensive simulations performed.

A. Motor Actuator Model

For the development of this system model, a model of the motor actuator used to power the waist joints was required. Equations (1) and (2) characterize a general DC motor.

$$J \frac{d^2\theta}{dt^2} = T - B \frac{d\theta}{dt} \Rightarrow \frac{d^2\theta}{dt^2} = \frac{1}{J} \left(K_t i - B \frac{d\theta}{dt} \right) \quad (1)$$

$$L \frac{di}{dt} = V - R \times i - e \Rightarrow \frac{di}{dt} = \frac{1}{L} \left(V - R \times i - K_e \frac{d\theta}{dt} \right) \quad (2)$$

This mathematical model was implemented using MATLAB Simulink, Figure 3, and the results were referenced with the real system.

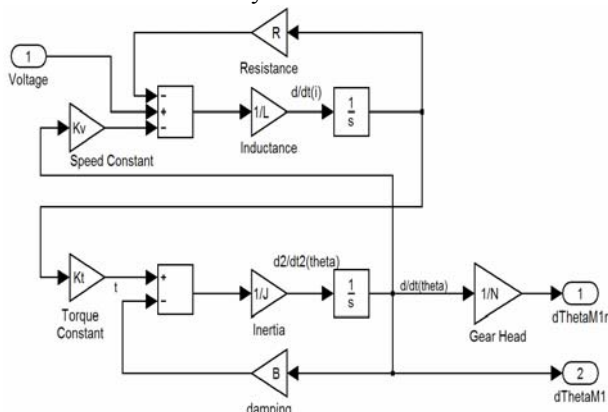


Fig. 3. MATLAB Simulink representation of the mathematical model of the two DC motors used to drive the differential waist mechanism.

B. Differential Mechanism Model

There are 2 motors controlling the pitch and roll motion

of the robot waist, both located in parallel one in front of the other, but with its shafts pointing in opposite directions. From the kinematics analysis of the joints, the differential equations for the differential driver are:

$$R \times (\theta_{M1} + \theta_{M2}) = \theta_{roll} \quad (3)$$

$$R \times (\theta_{M1} - \theta_{M2}) = \theta_{pitch} \quad (4)$$

Where R is the gear head reduction ratio for motor 1 and 2, θ_{M1} and θ_{M2} are the rotor angles for motor 1 and 2 respectively and θ_{roll} and θ_{pitch} are the waist roll and pitch rotation angles.

C. Waist Dynamics

In order to have an accurate mathematical description of the system the dynamics of the system must be included in the simulation; this includes the weights of the mechanical assembly, friction of the contact joints and motors and the inertia of the system. In Figure 4 the block named ‘‘spine dynamics’’ includes the waist kinematics (combines the motion of the two DC motors in differential mode) and the dynamics of a generic limb with a variable weight used to perform a wide range of tests under different sets of conditions.

D. Complete System Modelling

In the simulations performed, the position feedback is calculated by integrating the speed output from the DC motor model, in the real system the speed is calculated using the derivative of the position output acquired from incremental encoder readings. Figure 4 shows the final control scheme including the differential equations block and the system dynamics for both motors, for a 2 DOF motion.

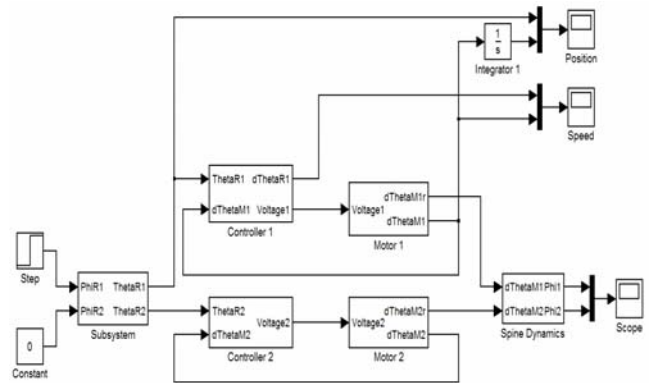


Fig. 4. Complete system for the 2 DOF differential joint. Speed and position control of 2 DC motors configured as a differential drive.

V. CONTROL SYSTEM

Many different approaches exist for control, each one with advantages and disadvantages, but the classic PID control scheme is still implemented in about 90% of real systems [18]. In this section, the design, model and simulation of a dual loop PID control system with a dynamic anti-windup scheme will be described.

A traditional PID controller uses the derivative and integral of the error signal; but when the reference input changes, the tracking error changes rapidly. The derivative signal of the tracking error can generate shock on the system [18]. To avoid this, the controller proposed uses the derivative of the output signal as shown in Figure 5.

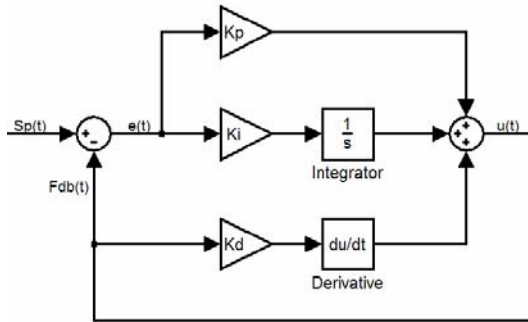


Fig. 5. Block Diagram of the classic three-term control scheme with derivative term using the feedback signal.

In order to perform position and speed control, a cascade controller was implemented. As observed in Figure 6 a first inner loop is used to control speed, this loop uses the position controller (outer loop) output as a reference signal. The speed is then established by setting the maximum and minimum values of the output limiter of the position controller. The fact that the speed is to be adjusted by setting a maximum and a minimum value to the limiter implies that the system will saturate. A simpler limiter will limit the position control output to a maximum value, which represents the desired maximum rotor speed. If this speed is low enough, the rotor can take a considerable amount of time to reach its final position, which in turn will produce a high integral term value.

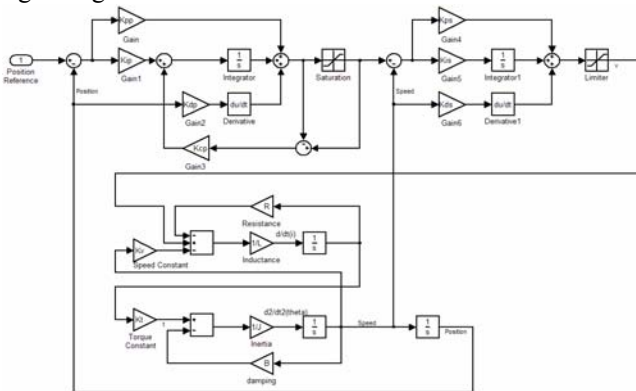


Fig. 6. Cascade control scheme for position and speed control, including the DC motor model.

In order to avoid this, a dynamic anti-windup scheme [18] was implemented; this scheme, Figure 7, takes the output of the system and compares it with a pre-saturated output to obtain a saturated error value, this value is then multiplied by a previously set gain and then introduced to the integrator, reducing its value. Using this scheme it is possible to ensure that the integral term will not have a high value so when the signal reaches its set point it will

effectively reduce the steady state error, further more reducing the overshoot. Figure 6 shows the mentioned scheme.

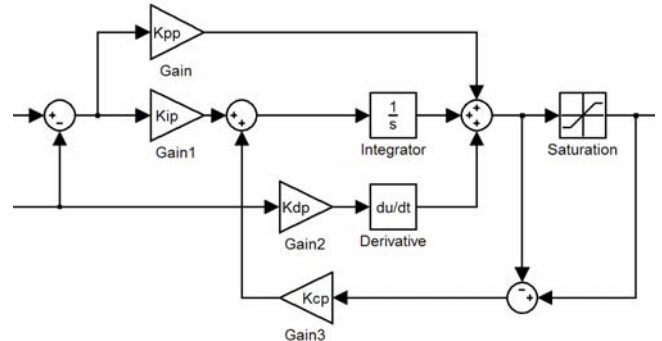


Fig. 7. Controller with dynamic anti-windup scheme, the integral term is effectively reduced, preventing overshoot and the saturation of the integral term.

VI. SIMULATION RESULTS

Testing of the control schemes were carefully evaluated and rigorously analyzed through simulations. For the following simulations, 2 types of reference signal were used: a step input signal and a sinusoidal signal at a range of different frequencies. In all cases, the solid lines represent the reference signals and the dashed lines the rotor position. In the following graphs, the only load considered was the weight of the limbs; the frictions in the joints were not considered.

A. Speed Control

The balance of the body of the robot is greatly affected by the speed of motion due to inertial forces generated by the body weight. The following graphs show the simulated results of the speed controller, with a forced reference input signal (the actual speed reference is generated by the position controller). These simulations were performed using MATLAB Simulink. The actuator groups used for this test consist of two MAXON DC motors and gearboxes with a maximum output speed after the reduction of 440 deg/s.

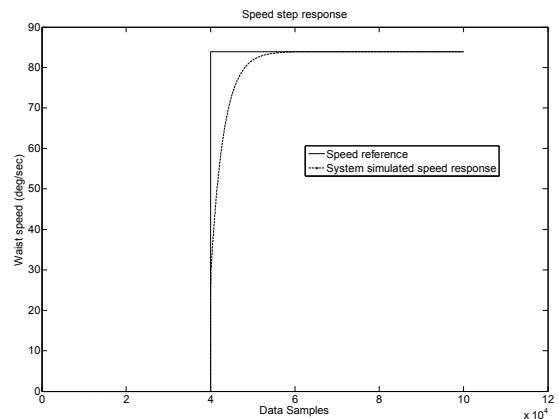


Fig. 8. Step response of the motor speed controller without load. This will help us evaluate the motor acceleration capabilities and the controller error margins.

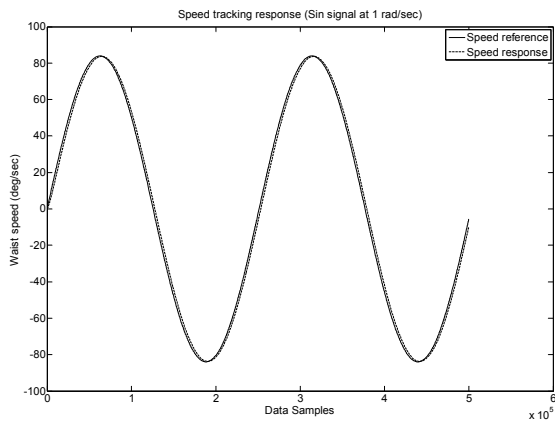


Fig. 9. With a 1 rad/s sinusoidal reference and a 1kg load over the joint.

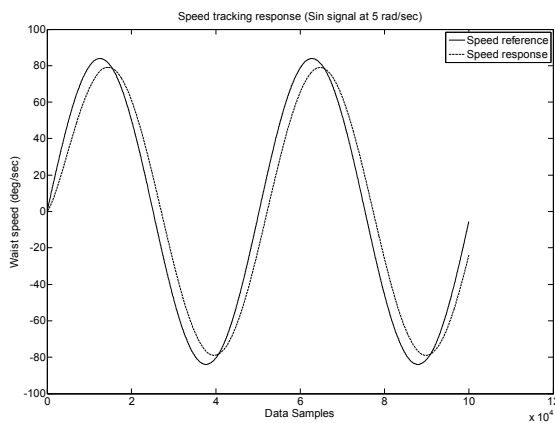


Fig. 10. With a 5 rad/s sinusoidal reference.

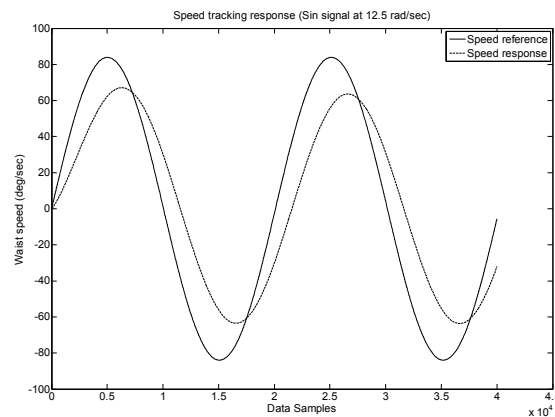


Fig. 11. With a 10 rad/s sinusoidal reference.

For the simulations results presented, reference signals of 84 deg/s (1.46 rad/s) were used and these represent the rotor speed for one of the motors.

This allowed the evaluation of the motor speed control capabilities under loaded and unloaded conditions and different motion directions (the load presented to the motor changes as the position of the centre of gravity of the robot's body moves) The simulation results shows a good speed response time capable of moving the body of the robot at acceptable speeds.

B. Position Control

The following graphs show the simulation results of the position using the complete model (position and speed controller cascaded).

The effect of a 1kg load in the tracking capabilities of the position controller can be seen; the load slows down the motion of the joint, even with a speed set near the motor maximum speed, though the position controller was able to position the waist joints with errors around 0.03deg in steady state.

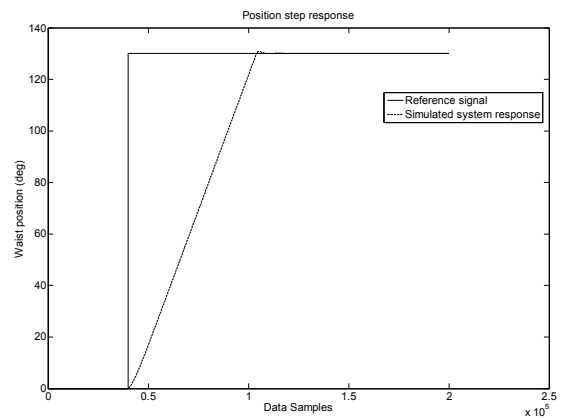


Fig. 12. Response for a square signal reference.

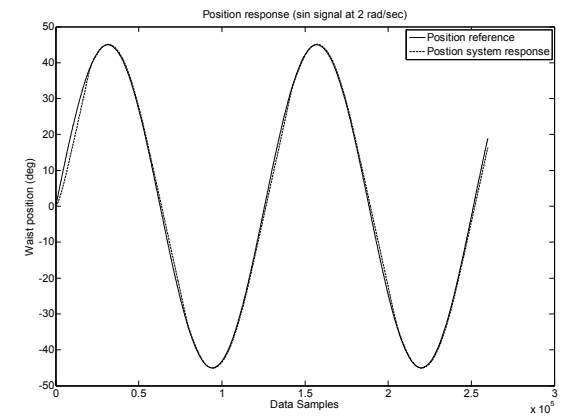


Fig. 13. Position tracking response with a 2 rad/s sinusoidal reference with a 90deg. of motion range.

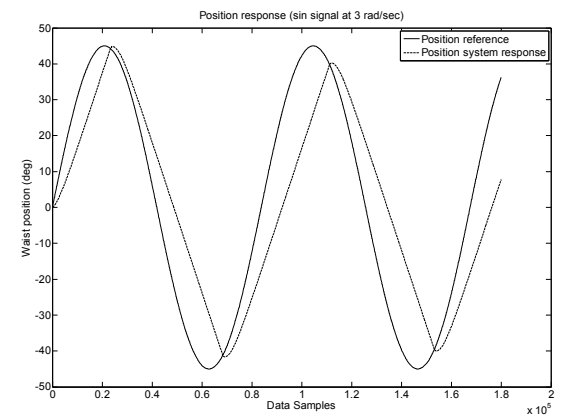


Fig. 14. Position tracking response with a 3 rad/s sinusoidal signal and 90deg of motion range.

Due to mechanical limitations, it can be observed from Figure 14 that the robot waist was not able to follow the reference signal accurately at rates of change higher than 2 rad/s even when setting the speed limit at its maximum.

VII. SYSTEM EXPERIMENTAL RESULTS

The following results were obtained by collecting measurements from the real system through the microcontroller (TMS320F2810, DSP from Texas Instruments) on which the control system was implemented, through its JTAG interface to a PC. Figure 15-17, show the results for the position control, when a step input is presented, with a set speed of 84 deg/s in the joint. The joint is set to move forward and backwards between 22 and 65 deg.

After evaluating the results from the real system, different factors not considered in the simulation model, like friction in the waist joints, were observed to have little effect on the results.

From the graphs below, errors of under 0.05deg in the position and under 1 deg/s for the speed can be observed.

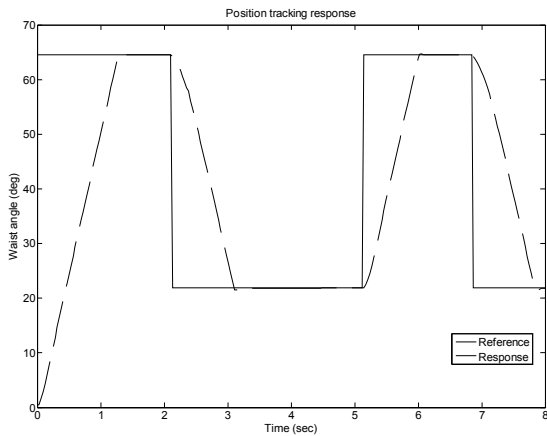


Fig. 15. Position Tracking Response of the real system. Reference signal in solid line, actual waist position in dashed line.

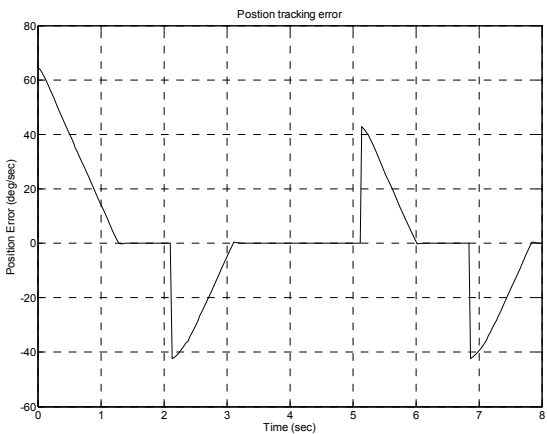


Fig. 16. Position tracking error of the real system.

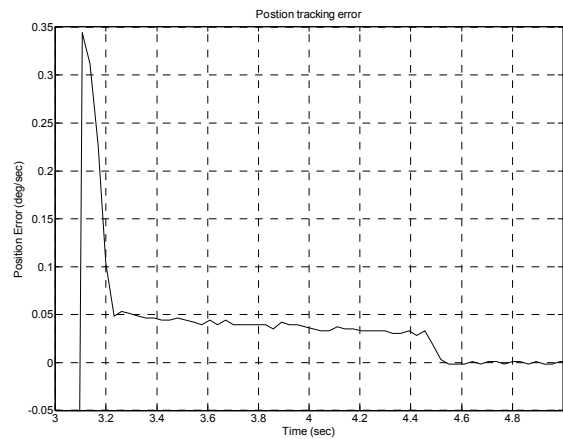


Fig. 17. Position tracking error. In this close up it is possible to observe the position error in steady state. Actual results show errors under 0.05deg in steady state with 0.35deg overshoot.

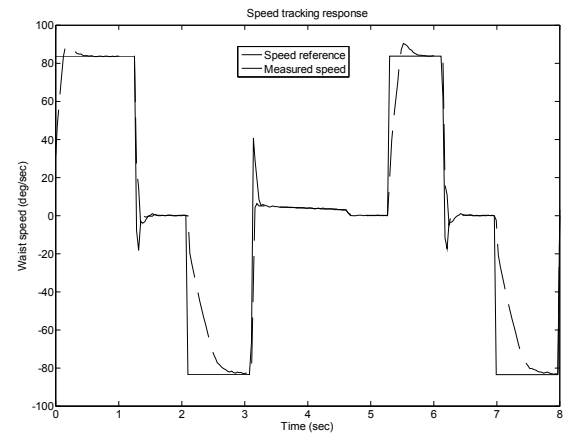


Fig. 18. Speed tracking response of the real system. Reference signal in solid line, actual waist speed in dashed line.

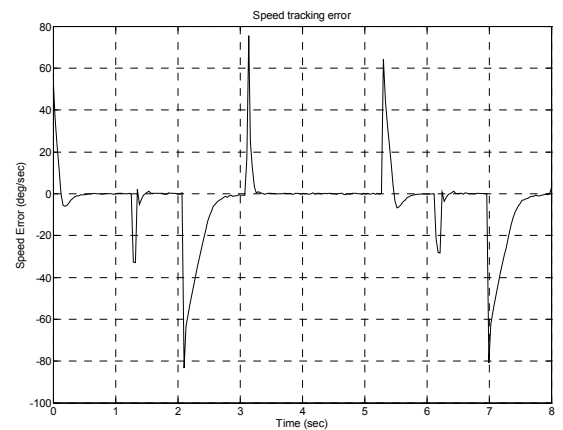


Fig. 19. Speed tracking error of the real system.

VIII. CONCLUSIONS AND FUTURE WORK

This work presented the design of a differential based mechanism developed to form the waist joint of a baby humanoid robot. A cascade PID based position and speed controller was developed and its characteristics, such as

overshoot, settling time and steady state error, have been evaluated through both experimentation and simulation. A control system consisting on a PID controller was established to achieve accurate position control of the joints.

It has been demonstrated through experimental implementation that the proposed control system can achieve control accuracy of 0.05 deg in step responses. In addition, a favorable speed control for sinusoidal and step trajectories was achieved. The control results presented in this study demonstrate that the proposed mechanism and control system can offer the desired motion range with high positional accuracy.

Future work will include a performance evaluation of the system using variable length and weight bodies to evaluate the effect of inertia on the system as well as mechanical (fatigue, maximum torques, etc.), electronic (current consumption, noise, etc.) and thermal effects.

ACKNOWLEDGMENT

This work is supported by the European Commission FP6, Project IST-004370. Special thanks also to Prof. D. G. Caldwell and Dr. N. Tsagarakis for their continuous support.

REFERENCES

- [1] J. Yamaguchi, E. Soga, S. Inoue, and A. Takanishi, "Development of a Bipedal Humanoid Robot – Control Method of Whole Body Cooperative Dynamic Biped Walking," Proc. IEEE Int. Conference on Robotics and Automation, pp. 368-374, 1999.
- [2] K. Nishiwaki, T. Sugihara, S. Kagami, F. Kanehiro, M. Inaba, and H. Inoue, "Design and Development of Research Platform for Perception-Action Integration in Humanoid Robot: H6," Proc. Int. Conference on Intelligent Robots and Systems, pp. 1559-1564, 2000.
- [3] K. Hirai, "Current and Future Perspective of Honda Humanoid Robot", Proc. IEEE/RSJ Int. Conference on Intelligent Robots and Systems, pp. 500508, 1997.
- [4] K. Hirai, M. Hirose, Y. Haikawa, and T. Takenaka, "The Development of Honda Humanoid Robot," Proc. IEEE ICRA, pp. 1321-1326, 1998.
- [5] M. Hirose, Y. Haikawa, T. Takenaka, and K. Hirai, "Development of Humanoid Robot ASIMO," Proc. Int. Conference on Intelligent Robots and Systems, Workshop2 (Oct.29, 2001), 2001.
- [6] M. Gienger, K. Löffler, and F. Pfeiffer, "Towards the Design of Biped Jogging Robot," Proc IEEE ICRA, pp. 4140-4145, 2001.
- [7] H. Inoue, S. Tachi, Y. Nakamura, K. Hirai, N. Ohyu, S. Hirai, K. Tanie, K. Yokoi, and H. Hirukawa, "Overview of Humanoid Robotics Project of METI," Proc. the 32nd Int. Symposium on Robotics, pp. 1478-1482, 2001.
- [8] K. Kaneko, F. Kanehiro, S. Kajita, K. Yokoyama, K. Akachi, T. Kawasaki, S. Ota, and T. Isozumi, "Design of Prototype Humanoid Robotics Platform for HRP," Proc. IEEE/RSJ Int. Conference on Intelligent Robots and Systems, pp. 2431-2436, 2002.
- [9] K. Kaneko, F. Kanehiro, S. Kajita, H. Hirukawa, T. Kawasaki, M. Hirata, K. Akachi, and T. Isozumi, "Humanoid Robot HRP-2", Proceedings of the 2004 IEEE ICRA, New Orleans, LA • April 2004
- [10] N. Kanehira, T. Kawasaki, S. Ota, K. Akachi, T. Isozumi, F. Kanehiro, and K. Kaneko, and S. Kajita, "Design and Experiment of Advanced Leg Module (HRP-2L) for Humanoid Robot (HRP-2) Development," Proc. Int. Conference on Intelligent Robots and Systems, 2002.
- [11] Satoru Shirata, Atsushi Konno, and Masaru Uchiyama, "Design and Development of a Light-Weight Biped Humanoid Robot Saika-4", Proc. IEEE/RSJ IROS, pp148-153, 2004, Sendai, Japan.
- [12] I. Mizuuchi, R. Tajima, T. Yoshikai, D. Sato, K. Nagashima, M. Inaba, Y. Kuniyoshi and H. Inoue, "The Design and Control of the Flexible Spine of a Fully Tendon-Driven Humanoid "Kenta", IEEE/RSJ IROS, pp2527-2532, 2002, Lausanne, Switzerland.
- [13] T. Furuta, Y. Okomura, and K. Tomiyama, "Design and Construction of a Series of Compact Humanoid Robots and Development of Biped Walk Control Strategies," Proc. IEEE-RAS Int. Conf on Humanoid Robots, 2000.
- [14] F. Yamasaki, T. Matsui, T. Miyashita, and H. Kitano, "PINO The Humanoid that Walks", Int. Conference on Humanoid Robots, 80.pdf, 2000.
- [15] Y. Kuroki, T. Ishida, J. Yamaguchi, M. Fujita, and T. Doi, "A Small Biped Entertainment Robot," Proc. IEEE-RAS Int. Conference on Humanoid Robots, pp. 181-186, 2001
- [16] Masahiro Fujita, Yoshihiro Kuroki, Tatsuzo Ishida, and Toshi T. Doi. Autonomous Behavior Control Architecture of Entertainment Humanoid Robot SDR-4X. In Proc. of IEEE/RSJ Int. Conf. on Intelligent Robots and Systems (IROS 2003), pp. 960-967, 2003.
- [17] Giorgio Metta, David Vernon, Giulio Sandini, "D8.1 Initial Specification of the CUB Open System", <http://www.robotcub.org>
- [18] K. J. Åström, "Advanced PID Control," ISA – The Instrumentation, Systems, and Automation Society, 2005.